DOI 10.2478/ama-2022-0020

NUMERICAL STUDY OF TRANSIENT ELASTOHYDRODYNAMIC LUBRICATION SUBJECTED TO SINUSOIDAL DYNAMIC LOADS FOR ROUGH CONTACT SURFACES

Mohamed F. ABD ALSAMIEH*

*Mechanical Design & Production Department, Military Technical College,
Ismail Al Fangari, El-Qobba Bridge, El Weili, Cairo, Egypt

mohamed.fahmy203@hotmail.com

received 22 August 2021, revised 23 November 2021, accepted 2 December 2021

Abstract: The purpose of this paper is to study the behaviour of transient elastohydrodynamic contacts subjected to forced harmonic vibrations, including the effect of surface waviness for concentrated counterformal point contact under isothermal conditions. Profiles of pressure and film thickness are studied to reveal the combined effects of sinusoidal external load and surface roughness on the lubrication problem. The time-dependent Reynolds' equation is solved using Newton–Raphson technique. The film thickness and pressure distribution are obtained at different snap shots of time by simultaneous solution of the Reynolds' equation and film thickness equation including elastic deformation and surface waviness. It is concluded that the coupling effects of the transient sinusoidal external load and wavy surface would result in increase in modulations of the pressure and film thickness profile in comparison to the case where the smooth contact surfaces are subjected to sinusoidal external load.

Key words: transient elastohydrodynamics, surface roughness, sinusoidal load, wavy surfaces

1. INTRODUCTION

Elastohydrodynamic lubrication is commonly known as a mode of fluid-film lubrication, in which the deformed surface and the pressure-dependent viscosity are taken into account to describe the formation of lubricant film. In fact, 90% of all machines and mechanisms comprise load-bearing and gear-transmitting contacts operating under elastohydrodynamic lubrication. However, it is generally known that machine elements operate under time-dependent conditions; therefore, the time-dependent motion of the elements results in transient lubrication. In such elements, the assumption of steady-state solution is inappropriate to study both film thickness and contact pressure to protect such components from direct contact and damage. In addition, the manufacturing processes of machine components cannot guarantee that the surfaces will be perfectly smooth; there will be imperfections on the surfaces, such as waviness. This imperfect surface may cause changes in the film thickness and pressure. The existence of such imperfections, however, may result in direct contacts of asperities once the film thickness is below a certain limit (see [1-3]).

Effect of transient conditions for elastohydrodynamic lubrication subjected to variation of load has been studied both experimentally and numerically in the past. Experimental investigations using optical interferometry technique reported in [4-10] showed that an oil entrapment is formed during rapid increase of the load, and as the entrainment speed increases, this entrapment of oil is diminished. The behaviour of transient elastohydrodynamic lubrication subjected to vibration has been studied numerically by many researchers such as in [11-14]. Their results revealed the solution of transient contact conditions subjected to variation of load is completely different from steady-state solution, especially at a high value of amplitude and frequency of vibration.

In the past, longitudinal and transverse roughness of ridges was studied both theoretically and experimentally. A numerical solution for the moving of a sinusoidal single transverse ridge through elastohydrodynamic lubrication for line and point contact problem have been investigated by many researchers as shown in [15-16]. Experimental studies using optical interferometry of the moving of a single transverse ridge through circular elastohydrodynamic contact have been presented in [17-18]. Effect of geometrical characteristics of the ridge on the formation of lubricant film thickness for elastohydrodynamic lubrication of point contact problem under rolling/sliding conditions haven been studied both experimentally and numerically in [19-20]. They used a single flat-top transverse ridge and the results showed that the lubricant film thickness was mainly affected by the geometrical characteristics of the ridge. The passage of a single flat-top transverse ridge through elastohydrodynamic lubrication for point contact problem has been studied numerically using multigrid technique in [21]. Analytical solution for different surface features of rectangular, rounded bottom and triangular shape have been provided in [22-23]. The results revealed that, an optimal indentation profile should have a smooth shape with appropriate width and depth. Recently, the behavior of a single ridge passing through elastohydrodynamic lubrication for different ridge shape and size including; flat-top, triangular and cosine wave pattern to get an optimal ridge profile has been studied numerically [24]. The results showed that, the film thickness profile and the pressure distribution through the contact zone were mainly affected by the geometrical characteristics of the ridge.

However, in real applications, elastohydrodynamic contacts are subjected to variation of load, geometry or velocity of the

contacting surfaces, often with more than one of the parameters varying at the same time, making the prediction of the film thickness a very difficult problem, even if these variations are known, which is not usually the case. The analysis of such behaviour may provide some views of the local force on the surfaces, and thus lead to a more reasonable prediction of the stress fields. Influence of the sinusoidal varying loads due to vibrations on the film thickness and pressure profile of the isothermal, elastohydrodynamically lubricated point contact with a wavy surface have been numerically investigated in [25]. The results revealed that the external sinusoidal dynamic load induces the modulations on the film thickness and pressure profile. The waviness on one contacting surface causes changes in the elastohydrodynamic behaviours to become more pronounced.

In the present paper, a detailed numerical solution and analysis of the elastohydrodynamic contacts subjected to a harmonic variation of load as well as the waviness of surface is considered for concentrated counterformal point contact under isothermal conditions. The behaviour of the transient elastohydrodynamic of point contact problem was evaluated relative to film thickness and pressure distribution, and on that basis, a time-dependent Reynolds' equation is solved using Newton-Raphson technique with Gauss-Seidel iteration method. The current numerical results have been compared with the results of the numerical work reported in [25].

2. BACKGROUND THEORY

The time-dependent Reynolds' equation can be written in a dimensionless form as:

$$\frac{\partial}{\partial X}\left(\frac{\bar{\rho}H^3}{\bar{\eta}}\frac{\partial P}{\partial X}\right)+\frac{\partial}{\partial Y}\left(\frac{\bar{\rho}H^3}{\bar{\eta}}\frac{\partial P}{\partial Y}\right)=\emptyset\left\{\frac{\partial(\bar{\rho}H)}{\partial X}+\frac{bE'}{\eta_0 u}\left(\bar{\rho}\frac{\partial H}{\partial \bar{t}}+H\frac{\partial \bar{\rho}}{\partial \bar{t}}\right)\right\} \quad (1)$$

The following dimensionless variables apply:

$$X=\frac{x}{b}, Y=\frac{y}{b}, \bar{\eta}=\frac{\eta}{\eta_0}, H=\frac{hR}{b^2}, P=\frac{p}{P_{Her}}, \phi=\frac{12R^2\eta_0 u}{b^3 P_{Her}}.$$

The film thickness is described in a dimensionless form as:

$$\Delta P_{k,l}^n = \frac{\left(-F_{i,j}-J_{k-1,l}^{i,j}\Delta P_{k-1,l}^n-J_{k+1,l}^{i,j}\Delta P_{k+1,l}^{n-1}-J_{k,l-1}^{i,j}\Delta P_{k,l-1}^n-J_{k,l+1}^{i,j}\Delta P_{k,l+1}^{n+1}\right)}{J_{k,l}^{i,j}}$$

where: $J_{k,l}^{i,j}=\frac{\partial F_{i,j}(t)}{\partial P_{k,l}}$ (2)

where *m* and *l* are the inlet boundaries in both the rolling and lateral directions, respectively, $H_o(T)$ is the dimensionless initial central film thickness, b is the radius of Hertzian contact region and $\delta(X,Y,T)$ is the total elastic deformation (see [1, 14 and 26]) and is given as

$$\delta_{I,J}(x,y)=\frac{2}{\Pi}\frac{P_{Her}}{E'}\sum_{j=1,2i=1,2}^{ny}\sum^{nx}P_{i,j}D_{i^*,j^*}$$

where *D* is the contact influence coefficient matrix and is given in [27].

The last term in equation (2), *S.R(X,Y,T)*, represents the geometry of the surface roughness and is given as:

$$S.R(X,Y,T)=\begin{cases}0 & X\geq X_d\\ Asin\left(2\pi\frac{X-X_d}{\lambda}\right) & X<X_d\end{cases}$$

where *A* is the dimensionless amplitude, λ is the dimensionless wavelength of the ridge and X_d is the dimensionless position of the located ridge through the contact zone and is given as $X_d={}^{x_d}/_{b}$, $x_d=x_0+ut$, x_0 is the initial position of the ridge at t = 0.

The variation of density with pressure was shown in [28] as:

$$\overline{\rho}=1+\frac{\varepsilon PP_{Her}}{1+\zeta PP_{Her}} \quad (3)$$

where ε and ζ are constants dependent upon the type of lubricant used.

The relation of viscosity with pressure was given in [29] as:

$$\overline{\eta}=exp[ln\eta_o+9.67]\lfloor(1+5.1*10^{-9}PP_{Her})^Z-1\rfloor \quad (4)$$

where *z* is the viscosity-pressure index and is given as:

The Reynolds' equation (1) can be solved using Newton-Raphson method in the following numerical form:

$$\sum_{l=2}^{N}\sum_{k=2}^{M}\frac{\partial F_{i,j(t)}}{\partial P_{k,l}}\Delta P_{k,l}=-F_{i,j}(t) \quad (5)$$

Using the Gauss–Seidel iteration method, equation (5) can be written as:

$$\Delta P_{k,l}^n = \frac{\left(-F_{i,j}-J_{k-1,l}^{i,j}\Delta P_{k-1,l}^n-J_{k+1,l}^{i,j}\Delta P_{k+1,l}^{n-1}-J_{k,l-1}^{i,j}\Delta P_{k,l-1}^n-J_{k,l+1}^{i,j}\Delta P_{k,l+1}^{n+1}\right)}{J_{k,l}^{i,j}}$$

where $J_{k,l}^{i,j}=\frac{\partial F_{i,j(t)}}{\partial P_{k,l}}$,

where *n* is the iteration counter.

The pressure can be updated according to the equation:

$$P_{i,j}^n=P_{i,j}^{n-1}+\Omega\Delta P_{i,j}^n \quad (6)$$

where Ω is an under-relaxation factor, which ranges from 0.05 to 0.1.

The external load variation (*W(t)*) is balanced by the integration of oil pressure distribution. The instantaneous load equation can be written as:

$$\iint_{-\infty}^{\infty}p(x,y,t)dxdy=W(t) \quad (7)$$

The convergence criteria for the pressure and load balance equations are:

$$\left[\frac{\sum_{j=1,2,..}^{N}\sum_{i=1,2,..}^{M}\left(P_{i,j}^n-P_{i,j}^{n-1}\right)^2}{MxN}\right]^{0.5}\leq 10^{-3} \quad (8)$$

$$\left|\iint P(X,Y)dXdY-\frac{2}{3}\pi\right|\leq 10^{-3} \quad (9)$$

where M and N are the total nodal points in both the *X*- and *Y*-directions, respectively.

3. RESULTS AND DISCUSSION

In this section, the steady and transient contact pressure distributions and film thickness profiles of elastohydrodynamic lubrication for smooth and wavy surface subjected to harmonic forced vibrations are presented to demonstrate the substantial impact of the dynamic response on the elastohydrodynamic behaviour for both wavy and smooth surfaces. The materials, lubricant properties and operating parameters of the numerical solution presented in [25] are listed in Table 1 and are used in the current numerical solution. They developed a simple transient elastohydrodynamic

point contact solver to solve the Reynolds' equation using Jacobi relaxation scheme for solving the pressure, and along with the half-space theory for solving the film thickness equation, which has been found to be suitable at low external loads and low speeds of entraining motion. At higher values of load and particularly moderate to high speeds of entraining motion, it is more appropriate to use Newton–Raphson technique with Gauss–Seidel iteration method. In the current analysis, Newton–Raphson technique with Gauss–Seidel iteration method has been used to solve the Reynolds' equation.

Tab. 1. Lubricant, material properties and operating parameters

Viscosity, η_0	0.0835 Pa s	Equivalent Young's modulus, E'	116.87 × 10^9 Pa
Viscosity coefficient, α	1.95 × 10^{-8} Pa^{-1}	Load	20 N
ε	5.83 × 10^{-10}	Speed	1 m/s
ξ	1.68 × 10^{-9}	Ball radius, R	0.01 m
Surface roughness amplitude, A	0.024 μm	Wavelength of the ridge, λ	0.27 mm

Figure 1 shows the steady-state film thickness and pressure distribution for the smooth contacting surfaces along X-direction presented by the current numerical solution. A load of 20 N and rolling speed of 1 m/s result in the maximum Hertzian dry contact pressure of 0.51 GPa with 0.136 mm radius of Hertzian contact region. It can be observed that all familiar features of elastohydrodynamic point contact are displayed, where pressure distribution is almost semi-ellipsoid and the pressure spike occurs at the exit region as well as the well-known horse shoe shape in the film shape appears. The central film thickness is nearly flattened, and the minimum film thickness is found in the side lobes of the horse shoe shape. It is clear that, the pressure and film thickness presented in Figure 1 turn out to be fairly consistent with those presented in [25].

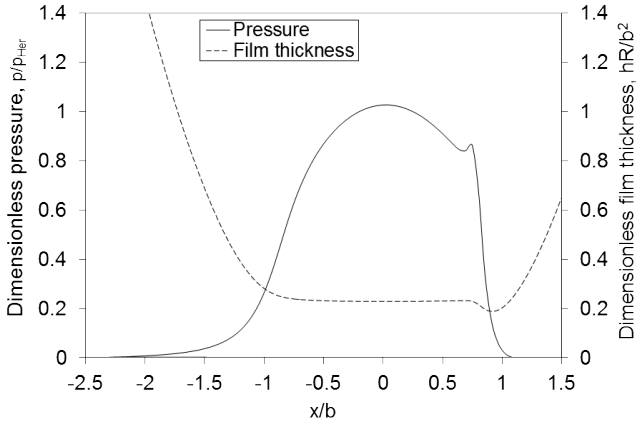

Fig. 1. Pressure and film thickness profile for the steady state of smooth surfaces

In order to investigate the effect of wavy surface for the steady-state elastohydrodynamic behaviors, a sinusoidal wavy surface with 0.024 μm amplitude and 0.27 mm wavelength is considered. Figure 2 shows the influence of waviness on the film thickness and pressure profile. It is clear that the pressure profile is no longer semi-ellipsoid in the contact area due to waviness and the film thickness profile is no longer flattened through the central contact region, in comparison to the case of smooth contact surface shown in Figure 1. The waviness on one contacting surface is almost completely deformed in the contact area, due to the high pressure in this contact area. The same conclusion was given in [25] for the same operating conditions.

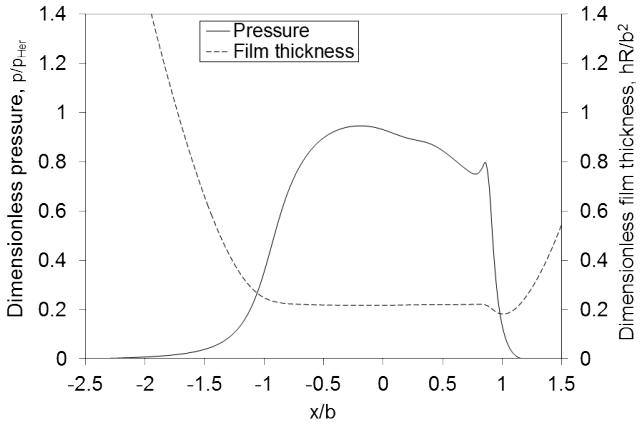

Fig. 2. Pressure and film thickness profile for the steady state of wavy surfaces

The effect of changes in the applied load due to external sinusoidal dynamic load on the pressure and film thickness profile is shown in Figure 3 for the case of smooth contacting surfaces. In fact, in the current analysis, it is assumed that the load varies between zero and a given value of 20 N in a sinusoidal fashion as expressed by:

$$W(t) = W_0 + a \times Sin(\omega t)$$

where, w_0 is the initial load and a is the amplitude of the sinusoidal load. The numerical solutions are carried out at 2π dimensionless frequency excitation.

Figure 3 shows the pressure and film thickness profile in the central line of contact along the rolling direction at different snapshots of time. It is clear that propagation in the pressure and film thickness from the inlet towards the outlet of the contact due to dynamic load is observed, although the contacting surfaces are assumed to be perfectly smooth. From Figure 3, it is clear that the modulation in the pressure and film thickness profile is periodic since the external dynamic load applied to the contact changes sinusoidally. The film thickness and pressure profile at t = 2.5 s (see Figure 3 f) are coincident with those at t = 1.0 s (see Figure 3 c), and the film thickness and pressure profile at t = 3.0 s (see Figure 3 g) are coincident with those at t = 1.5 s (see Figure 3 d). It is obvious that initially, the pressure and film thickness profile exhibit the classic flat film shape through the whole contact zone, which characterises the steady-state film behaviour (see Figure 3 a). The modulation of pressure and film thickness profile induced by the harmonic applied load is shown in Figure 3 b – d. The modulation in film thickness and pressure profile due to the action of harmonic external applied load, which is shown in Figure 3 e – h, is coincident to that shown in Figure 3 a –d since the external dynamic load applied to the contact changes sinusoidally. These results conform well to the results presented by other authors like in [25].

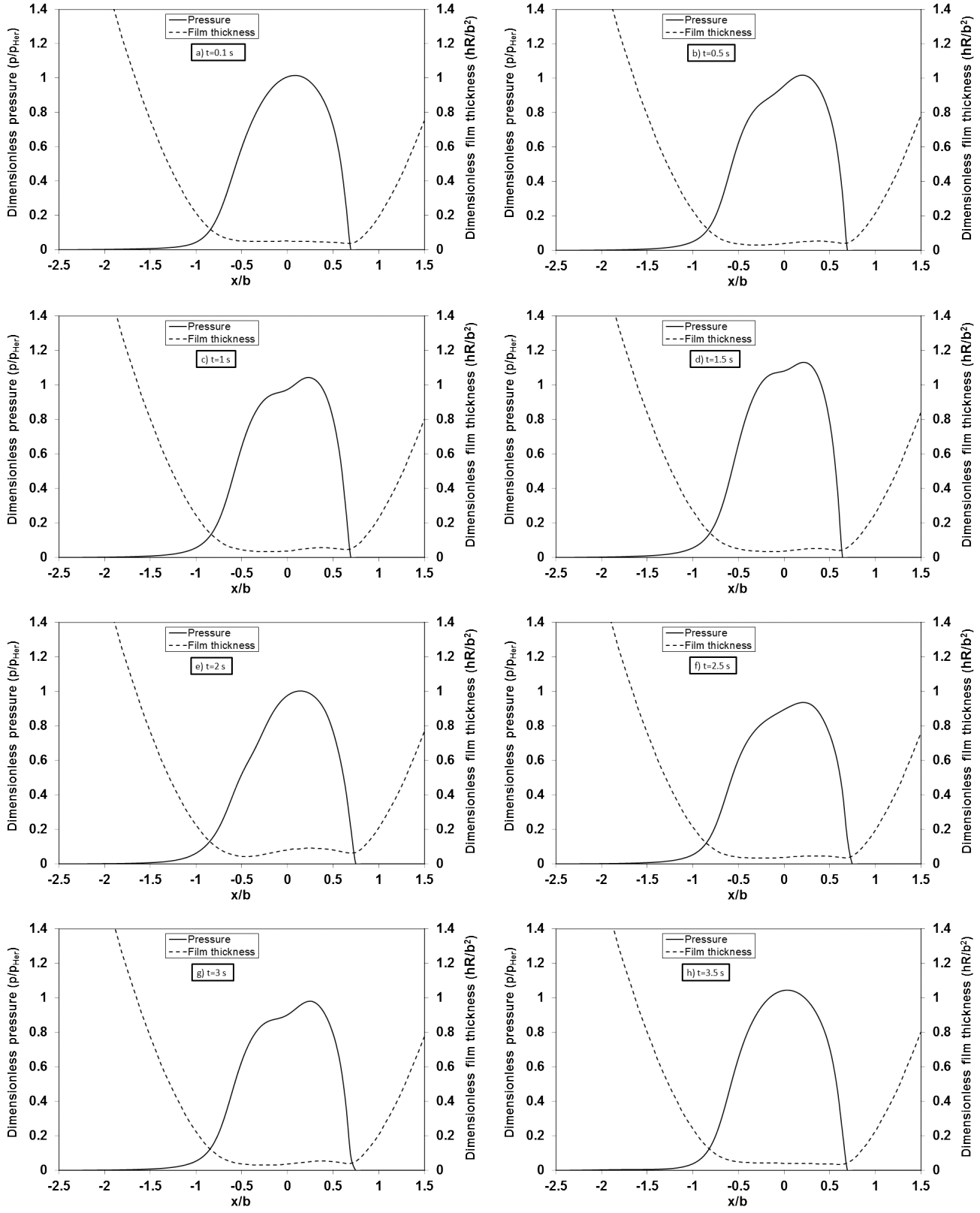

Fig. 3. Film shape and pressure profile in the central line of contact for smooth contacting surfaces

Finally, the combined effects of rough surface elastohydrodynamic lubrication contact subjected to the sinusoidal dynamic load are studied. In this case, a sinusoidal wavy surface and a sinusoidal dynamic load are considered to show their effects on pressure and film thickness profile. Figure 4 shows the changes in the central line pressure and film thickness profile along the X-direction at different snap-shots of time. It is clear that surface waviness causes fluctuations in pressure and film thickness within the nominal contact zone similar to the case of smooth contacting surfaces. Under these conditions, more evident fluctuations in pressure and film thickness profile are observed. However, due to the waviness onto one surface, the modulations of film thickness

DOI 10.2478/ama-2022-0020

and pressure profile are no longer periodic as in the case of smooth contact surface. The same feature was found in the numerical solution presented in [25] for elastohydrodynamic lubrication of point contact problem.

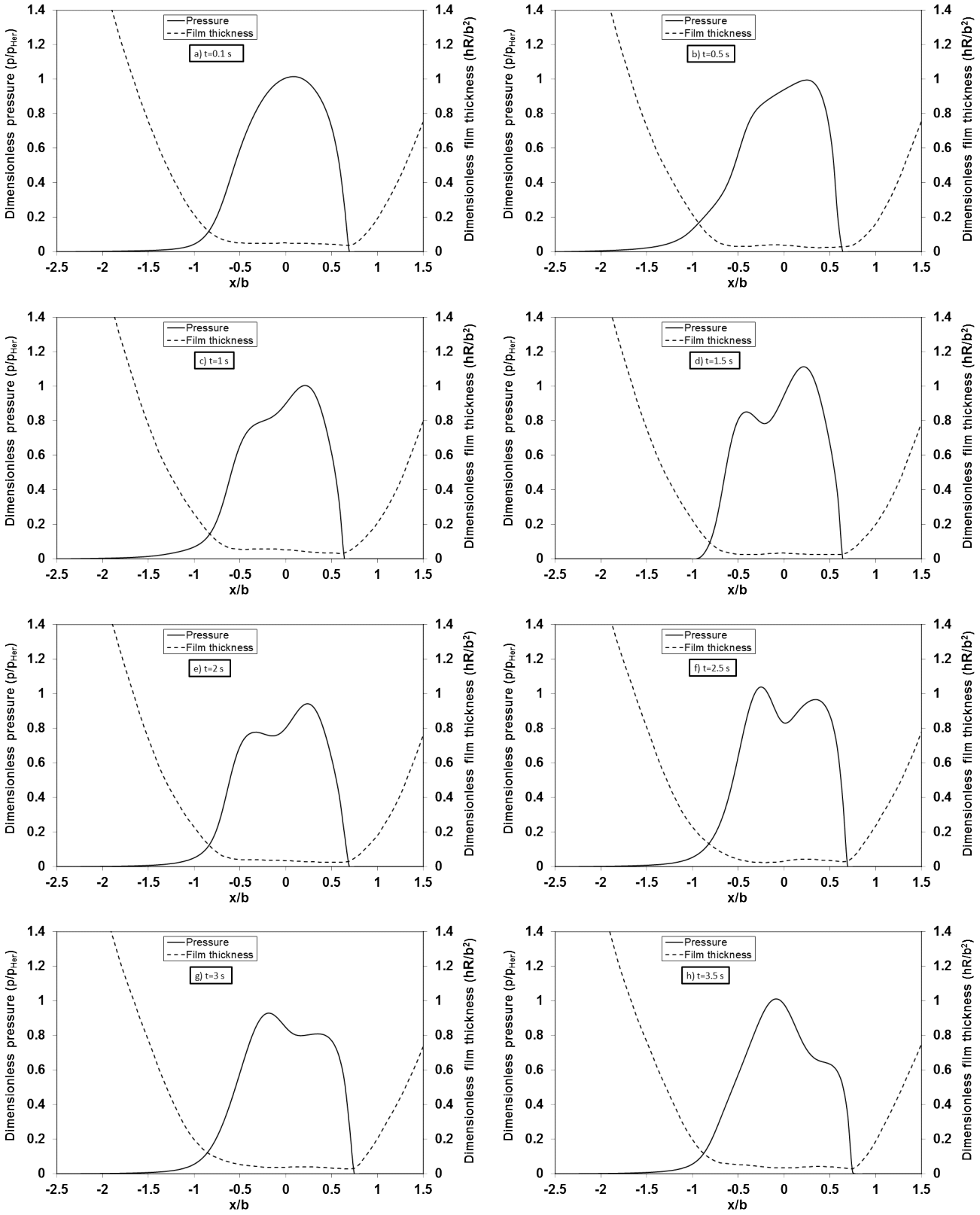

Fig. 4. Film shape and pressure profile in the central line of contact for wavy contacting surfaces

Unfortunately, there is no existing other previous numerical or experimental work in the area of elastohydrodynamic lubrication problem where the wavy surface contacts are subjected to harmonic forced vibrations to compare with. This is an area requiring

more research because in real applications, contacts are subjected to variations in load, speed and geometry at the same time, and it is hoped that this investigation and others will trigger further work.

4. CONCLUSIONS

The response of the elastohydrodynamic lubricated contacts subjected to combined effects of harmonic forced vibrations and waviness of contacting surfaces is discussed in this paper using a numerical technique based on Newton–Raphson with Gauss–Seidel iteration method for concentrated counterformal point contact under isothermal conditions. The results of the current numerical solution are compared with the numerical work presented by other researchers for steady and transient problem conditions for smooth and wavy contacting surfaces. The numerical results showed that the external dynamic load induces modulations in the film thickness and pressure profile in the lubricated contact. The combined effects of contacting surface waviness and external dynamic load cause more pronounced modulations in the pressure and film thickness profile in comparison to the case of external dynamic load. This result is supported by the numerical work presented by other researchers which showed a good agreement between both sets of results for all loading and contacting surface conditions.

REFERENCES

1. Gohar R, Rahnejat H. Fundamentals of tribology. Imperial College Press, London; 2008.
2. Simon V. Optimal tooth modifications in face-hobbed spiral bevel gears to reduce the influence of misalignments on elastohydrodynamic lubrication. ASME J Mech. Des. 2014; 136(7):1-9.
3. Simon V. Improvements in the mixed elastohydrodynamic lubrication and in the efficiency of hypoid gears. Proceeding of the IMechE, Part J: Journal of Engineering Tribology. 2019; 324(6):795-810.
4. Wijnant YH, Venner CH, Larsson R, Ericsson P. Effects of structural vibrations on the film thickness in an EHL circular contact. Trans. ASME, J. Trib. 1999; 121(2):259-264.
5. Kilali TEl, Perret-Liaudet J., Mazuyer D. Experimental analysis of a high pressure lubricated contact under dynamic normal excitation force. Trans. Proc. Trib., Proc. Of the 30thLeeds-Lyon Symp. on Tribology. 2004:409-418.
6. Sakamoto M, Nishikawa H, Kaneta M. Behavikaor of Point Contact EHL Films Under Pulsating Loads. Trans. Proc. Trib., Proc. Of the 30thLeeds-Lyon Symp. on Tribology. 2004:391-399.
7. Kalogiannis K, Mares C, Glovnea RP, Ioannides E. Experimental investigation into the Response of Elastohydrodynamic Films to Harmonic Vibrations. International Journal of Mechatronics and Manufacturing Systems. 2011; 4(1):61-73.
8. Zhang X, Glovnea RP. The Behaviour of Lubricated EHD Contacts Subjected to Vibrations. IOP Conf. Ser.; Mater. Sci. Eng. 2017;174.
9. Glovnea RP, Zhang X, Sugimura J. The Effect of Lubricant Supply and Frequency upon the Behaviour of EHD Films Subjected to Vibrations. IOP Conf. Ser.; Mater. Sci. Eng. 2017;174.
10. Glovnea RP, Zhang X. Elastohydrodynamic Films under Periodic Load Variation: An Experimental and Theoretical Approach. Tribology Letters. 2018; 66(3):1-11.
11. Yang P, Cui J, Jin JM, Dowson D. A theoretical study on the response of a point elastohydrodynamic lubrication contact to a normal harmonic vibration under thermal and non-Newtonian conditions. Proc. IMechE, Part C. 2007; 221(9):1089-1110.
12. Morales-Espejel GE. Central film thickness in time-varying normal approach of rolling elastohydrodynamically lubricated contacts. Proc. IMechE, Part C. 2008; 222(7):1271-1280.
13. Felix-Quinonez A, Morales-Espejel GE. Film thickness fluctuations in time-varing normal loading of rolling elastohydrodynamically lubricated contacts. Proc. IMechE, Part C. 2010; 224(12): 2559-2567.
14. Al-Samieh MF. Numerical investigation of Elastohydrodynamic contacts subjected to harmonic load variation. Industrial Lubrication and Tribology. 2019; 71(6):832-841.
15. Venner CH, Lubrecht AA. Numerical simulation of a transverse ridge in a circular EHL contact, under rolling/sliding. Trans. ASME, J.Tribology. 1994; 116(4):751-761.
16. Holmes MJA, Evans HP, Hughes TG, Snidle RW. Transienelasto-hydrodynamic point contact analysis using a new coupled differential deflection method Part 1: Theory and validation. Proceeding of the IMechE, Part J: Journal of Engineering Tribology. 2003; 217(4): 289-303.
17. Glovnea RP, Choo JW, Olver AV, Spikes HA. Compression of a single transverse ridge in a circular elastohydrodynamic contact. ASME Journal of Tribology. 2003; 125(2):275-282.
18. Armando FQ, Pascal E, Jonathan LS. New experimental results of a single ridge passing through an EHL conjunction. ASME Journal of Tribology. 2003; 125(2):252-259.
19. Felix-Quinonez A, Ehret P, Summers JL. Numerical analysis of experimental observations of a single transverse ridge passing through an elastohydrodynamic lubrication point contact under rolling/sliding conditions. Proceeding of the IMechE, Part J:Journal of Engineering Tribology. 2004; 218(2):109-123.
20. Felix-Quinonez A, Ehret P, Summers JL, Morales-Espejel GE. Fourier analysis of a single transverse ridge passing through an elastohydrodynamically lubricated rolling contact: a comparison with experiment. Proceeding of the IMechE, Part J: Journal of Engineering Tribology. 2004; 218(1):33-43.
21. Ildiko F, Sperka P, Hartl M. Transient calculations in elastohydrodynamically lubricated point contacts. Engineering Mechanics. 2014; 21(5):311–319.
22. Sperka P., Krupka I. and Hartl M. Rapid prediction of roughness effects in sliding EHL contacts. STLE Annual Meeting & Exhibition, Michigan, USA. 2013; May 5-9.
23. Sperka P, Krupka I, Hartl M. Prediction of Shallow Indentation Effects in a Rolling-Sliding EHL Contact Based on Amplitude Attenuation Theory. Japanese Society of Tribologists. 2017; 12(1):1-7.
24. Al-Samieh MF. Effect of changing geometrical characteristics for different shapes of a single ridge passing through elastohydrodynamic of point contacts. Industrial Lubrication and Tribology. 2021; 73(2):283-296.
25. Cupu DRP, Stratmann A, Jacobs G. Analysis of transient elasto-hydrodynamic lubrication of point contact subjected to sinusoidal dynamic loads. International Conference on Design, Energy, Materials and Manufacture, IOP Conf. Series: Materials Science and Engineering 539. 2019.
26. Al-Samieh MF. Theoretical Investigation of Transient Ultra-Thin Lubricant Film during rapid deceleration. Tribology in industry. 2018; 40(3): 349-357.
27. Johnson KL. Contact mechanics. Cambridge University Press. 1985; Chapter 3: 54.
28. Dowson D, Higginson GR. A numerical solution to the elastohydrodynamic problem. J. Mech. Engng. Sci. 1959; 1(1):6-15.
29. Roelands CJA. Correlation aspects of viscosity-temperature-pressure relationship of lubricating oils. PhD thesis. Delft University of Technology, The Netherlands. 1966.

Mohamed F. Abd Alsamieh: https://orcid.org/0000-0001-9308-8897

Nomenclature

A	Dimensionless surface roughness amplitude	Z	Viscosity-pressure index
B	Radius of Hertzian contact region	α	Viscosity coefficient
E'	Equivalent Young's modulus	δ	Total elastic deformation
G^*	Materials' parameter, $G^* = E' \alpha$	η	Lubricant viscosity
h	Lubricant film thickness	η_0	Atmospheric lubricant viscosity
H	Dimensionless film thickness, $H = hR/b^2$	ρ	Lubricant density
H_0	Dimensionless central film thickness	ρ_o	Atmospheric lubricant density
p	Pressure	$\overline{\rho}$	Dimensionless lubricant density, $\overline{\rho} = \rho / \rho_0$
P	Dimensionless pressure, $P = p/P_{Her}$	$\overline{\eta}$	Dimensionless lubricant viscosity, $\overline{\eta} = \eta / \eta_0$
N, M	Total number of mesh points in X- and Y- directions	λ	Dimensionless wavelength of the ridge
R	Radius of contact	$S.R$	Surface roughness
W	Normal applied load	Superscripts	
X,Y	Dimensionless coordinates, $X = x/b$, $Y = y/b$	i,j	Contravariant influence coefficient indices
u	Rolling speed, $u = (u_A + u_B)/2$	n	Iteration index
U^*	Speed parameter, $U^* = u\eta_o/E'R_2$	k,l	Covariant influence coefficient indices